ACS Photonics

Article

pubs.acs.org/journal/apchd5

Nonlinear Optical Response of Organic–Inorganic Halide Perovskites

Rui Zhang,[†,#] Jiandong Fan,[‡,#] Xing Zhang,[§] Haohai Yu,[*,†] Huaijin Zhang,[*,†] Yaohua Mai,[§] Tianxiang Xu,[†] Jiyang Wang,[†] and Henry J. Snaith[*,‡]

[†]State Key Laboratory of Crystal Materials and Institute of Crystal Materials, Shandong University, Jinan 250100, China

[‡]Clarendon Laboratory, University of Oxford, Parks Road, Oxford OX1 3PU, United Kingdom

[§]Institute of Photovoltaics, College of Physics Science and Technology, Hebei University, Baoding 071002, China

Supporting Information

ABSTRACT: Metal halide perovskites have exhibited excellent properties as absorbers in solar cells, but this may simply be the first of many applications for this intriguing class of materials. Here, we report the nonlinear optical response of triiodide ($CH_3NH_3PbI_3$) and mixed halide ($CH_3NH_3PbI_{3-x}Cl_x$) perovskite absorbers. The results show that they have large nonlinear refractive index (NRI), 3 orders of magnitude larger than that of silicon. Particularly, the NRI of $CH_3NH_3PbI_{3-x}Cl_x$ is more than two times larger compared to that of $CH_3NH_3PbI_3$. Meanwhile, both of them have been proven to possess saturable absorption effects with small nonlinear absorption coefficients which indicate that they can maintain excellent absorption under high-intensity irradiation and are favorable to modulators toward large-energy pulsed laser. Taking into consideration the saturable absorption effect, we demonstrated a pulsed laser with the perovskite as a pulse modulator. These results above indicate the potential for perovskites to be employed in nonlinear optoelectronic devices.

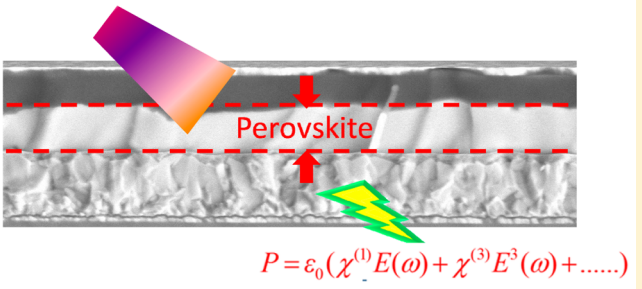

KEYWORDS: *metal halide perovskites, nonlinear optical response, Kerr effects, saturable absorption, pulse modulator*

Solar energy conversion is considered as one of the likely keys solutions to satisfy the growing global energy demand.[1−3] Recently, extremely rapid progress has been made in organic–inorganic halide perovskites solar cells with the energy conversion efficiencies already exceeding 20%,[4−11] and if they make commercial success, the discovery will be a revolutionary moment for the progress of photovoltaics. Nevertheless, despite the superb performances, perovskite solar cells suffer from some weak points which still require effort to overcome, i.e., instability against humidity and an anomalous hysteresis effect in the current voltage, most likely originating from drifting mobile ions and interfacial traps.[12]

In physics, the absorption of light in semiconductors such as the perovskites belongs to a light–matter interaction process in which the electrons in the interacted materials resonate with the electric field of the irradiating optical signal and induce polarization. In the simplest form, assuming the dielectric response in an isotropic material, the relation between a generated polarization P and an electric field $E(\omega)$ of the excitation optical signal with the circular frequency ω is expressed as[13]

$$P = \varepsilon_0(\chi^{(1)}E(\omega) + \chi^{(2)}E^2(\omega) + \chi^{(3)}E^3(\omega) + ...) \quad (1)$$

where ε_0 is the dielectric permittivity of the vacuum, $\chi^{(n)}$ is the nth-order susceptibility consisting of real and imaginary parts $\chi_r^{(n)}$ and $\chi_i^{(n)}$, respectively, and $\chi^{(n)}$ is several orders of magnitude larger than $\chi^{(n+1)}$. Therefore, under weak radiation such as terrestrial sun light, the polarization is proportional to the excitation electric field and $\chi^{(1)}$ is responsible for the linear optics such as linear absorption, emission, refraction, etc. In contrast, under higher levels of irradiation from sources such as lasers, nonlinear optical properties can be observed. In the linear optics, the bright light-emitting,[14] broadband photodetecting,[15] and random lasing[16] were reported concerning the organic–inorganic halide perovskites as gain materials, beside the intensive investigation on the solar cells.

Concerning the crystal structure, although there is some ambiguity over the precise space group due to imprecise determination of the position of the organic methylammonium (MA), $MAPbI_3$ perovskite is likely to be cento-symmetric[17,18] indicating $\chi^{(2)} = 0$ at room temperature. Therefore, third-order nonlinear optics may be generated under irradiation by high-intensity light. Besides discovering the nature of a material, third-order nonlinear optics, including $\chi_r^{(3)}$ and $\chi_i^{(3)}$, have been extensively applied in optoelectronics.[13] Thereby, considering the advantages such as low processing costs, the perovskites would play important roles in nonlinear optics and optical devices. In this scenario, there is no report concerning the nonlinear optical response of organic–inorganic halide perovskites, which might be associated with the anomalous hysteresis effect and guide the fabrication of optical devices. Here, we

Received: September 30, 2015
Published: January 25, 2016

DOI: 10.1021/acsphotonics.5b00563
ACS Photonics 2016, 3, 371−377

show the third-order nonlinear optics of triiodide ($CH_3NH_3PbI_3$) and mixed halide ($CH_3NH_3PbI_{3-x}Cl_x$) perovskites absorbers under high-intensity irradiation including visible and near-infrared lasers. Afterward, we demonstrate a promising application as a saturable absorber for modulating the laser operation. This work is likely to stimulate significant effort toward realizing these and similar perovskites as nonlinear materials in optoelectronics.

RESULT AND DISCUSSION

Nonlinear Optical Response of Metal Halide Perovskites. We measured the absorption spectrum of $CH_3NH_3PbI_3$ and $CH_3NH_3PbI_{3-x}Cl_x$ thin film, as 1 − log (transmission) with a V-570 JASCO UV/vis/NIR spectrophotometer and show the results in Figure 1. We observe absorption onset at around 800 nm for both samples which is associated with the optical band gap of perovskite thin films. At longer wavelengths, their absorption as the function of wavelength toward near-infrared region gradually decreased. There should be no optical transition between the valence and conduction band in the region longer than 800 nm.[18−20] Recently, the theoretical and experimental study about the organic−inorganic perovskites has discovered that there is a distribution of subgap trap states which are located under the conduction band,[21] account for the largest fraction of electron−hole recombination, and would expand the absorption range. Therefore, the absorption at the wavelength longer than 800 nm should be generated by the transition terminated to the subgap trap states, and also manifests that both $CH_3NH_3PbI_3$ and $CH_3NH_3PbI_{3-x}Cl_x$ should have potentially optoelectronic applications in the wavelength range shorter than at least 2000 nm.

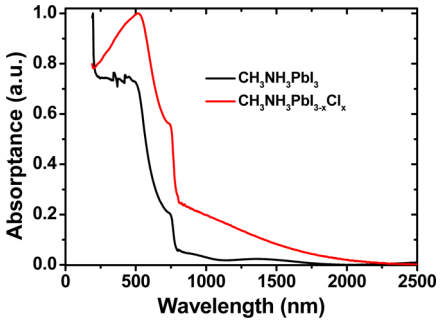

Figure 1. Absorption spectra of triiodide $CH_3NH_3PbI_3$ and mixed halide $CH_3NH_3PbI_{3-x}Cl_x$ perovskites.

We employed the Z-scan technique to investigate the nonlinear optical response of $CH_3NH_3PbI_3$ and $CH_3NH_3PbI_{3-x}Cl_x$ layers with a PY61 mode-locked neodymium doped yttrium aluminum garnet (Nd:YAG) laser (pulse width of 40 ps and wavelength of 1.06 μm) as the pump source. We show the configuration for Z-scan technique in Figure 2 and Supporting Information. The third-order nonlinear optics is contributed by the real part $\chi_r^{(3)}$ and the imaginary part $\chi_i^{(3)}$, which manifest as the NRI and nonlinear absorption as[22,23]

$$n = n_0 + \gamma I$$
$$\alpha = \alpha_0 + \beta I \quad (2)$$

with

$$\chi_r^{(3)} = 2n_0\varepsilon_0 c\gamma$$
$$\chi_i^{(3)} = \frac{n_0^2\varepsilon_0 c^2}{\omega}\beta \quad (3)$$

where n and α are the refractive index and absorption coefficient, respectively, under the laser intensity of I within the sample, n_0 is the linear refractive index, γ is the NRI, β is the nonlinear absorption coefficient, ε_0 is the permittivity in vacuum, c is the speed of light in vacuum, and ω is the optical frequency. With the transmission at weak irradiation as a standard, we measured the nonlinear absorption and NRI using open-aperture and close-aperture techniques, respectively. The

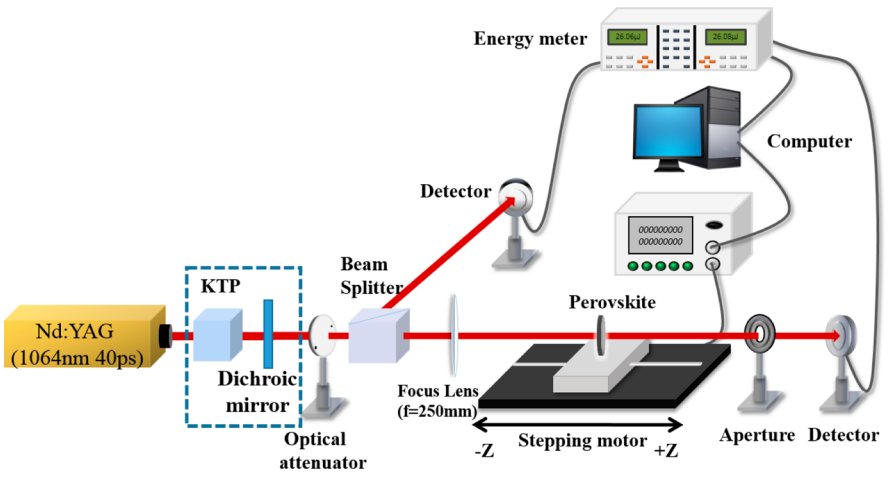

Figure 2. Experimental setup for Z-scan technique. A neodymium doped yttrium aluminum garnet (Nd:YAG) laser with the center wavelength of 1064 nm and pulse width of 40 ps was used as the pump source. The output energy from the Nd:YAG laser was tuned with an optical attenuator. With a beam splitter, the Nd:YAG laser was split into two beams. One beam was used as the reference and another beam was focused by an objective lens. The perovskite solar cell sample perpendicularly oriented toward the incident beam and can be moved along the z-axis with a linear motorized stage. Two energy meters were employed to simultaneously detect the optical energy from different branches. An aperture was inserted in front of the detector energy meter and used for the investigation of nonlinear transmission. For the experiments at 532 nm laser, a type II cut potassium titanium oxygenic phosphate (KTP) single crystal was inserted after the Nd:YAG laser for the second harmonic generation and a dichroic mirror was placed after KTP crystal for transmitting 532 nm laser and reflecting 1064 nm laser.

DOI: 10.1021/acsphotonics.5b00563
ACS Photonics 2016, 3, 371−377

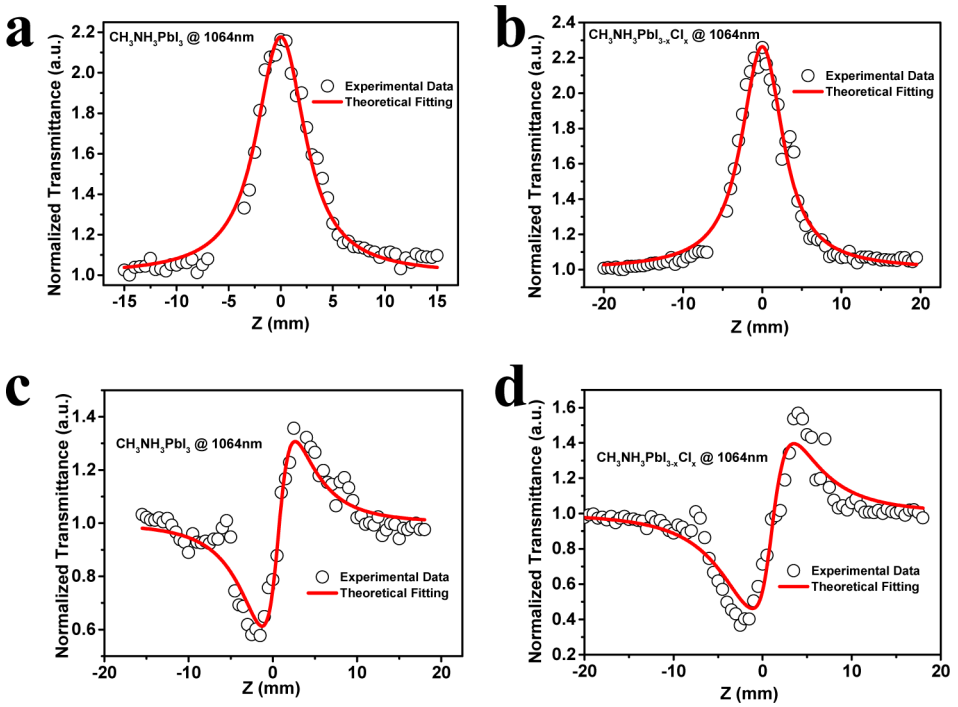

Figure 3. Nonlinear absorption of $CH_3NH_3PbI_3$ and $CH_3NH_3PbI_{3-x}Cl_x$ samples under irradiation of a 1064 nm pulsed laser. (a) Experimental results and theoretical fitting for the nonlinear absorption of $CH_3NH_3PbI_3$. (b) Experimental results and theoretical fitting for the nonlinear absorption of $CH_3NH_3PbI_{3-x}Cl_x$. (c) Experimental results and theoretical fitting for the nonlinear refractive index of $CH_3NH_3PbI_3$. (d) Experimental results and theoretical fitting for the nonlinear refractive index of $CH_3NH_3PbI_{3-x}Cl_x$.

Table 1. Comparison between Organic−Inorganic Absorbers with Si, GaAs, and Silica

	532 nm		1.06 μm		
samples	nonlinear absorption coefficient (β: cm/MW)	saturable intensity (I_{sat}: GW/cm^2)	nonlinear absorption coefficient (β: cm/MW)	saturable intensity (I_{sat}: GW/cm^2)	nonlinear refractive index (γ: $\times 10^{-15}$ m^2/W)
$CH_3NH_3PbI_{3-x}Cl_x$	−203.3	0.5	−2.03	12.61	8.36
$CH_3NH_3PbI_3$	−152	0.84	−2.25	12.71	3.74
$CH_3NH_3PbBr_3$ (Single Crystal)	/	/	8.2×10^{-3} (at 0.8 μm)[24]	/	/
Si	/	/	/	/	4.5×10^{-3}(at 1.55 μm)[13]
Silica	/	/	/	/	~2×10^{-5} (at 800 nm)[28−30]
GaAs	/	/	-9.4×10^{7} (at 1.55 μm)[24]	7.9×10^{-8} (at 1.55 μm)[24]	3.25×10^{-2} [27]

close aperture technique allows measuring the optical transmission change resulting from the combined consequence of the nonlinear absorption and nonlinear phase change induced by the NRI.

In the open aperture condition, we present the experimental results for the nonlinear transmission at the irradiation wavelength of 1064 nm in Figure 3, panels a and b for $CH_3NH_3PbI_3$ and $CH_3NH_3PbI_{3-x}Cl_x$, respectively. We find that the transmissions increase as the position of the samples approaches to the focused point $z = 0$, which indicates that both samples have saturable absorption properties. By theoretical fitting as shown in Supporting Information, we found that for $CH_3NH_3PbI_3$, the nonlinear absorption was $\beta = -2.25$ cm/MW with the saturable intensity $I_{sat} = 12.71$ GW/cm^2, and for $CH_3NH_3PbI_{3-x}Cl_x$, nonlinear absorption was $\beta = -2.03$ cm/MW with the saturable intensity $I_{sat} = 12.61$ GW/cm^2, which is very similar to that of $CH_3NH_3PbI_3$. The saturable absorption intensity of the two samples is about 10^8 times larger than that of gallium arsenide (GaAs) (79 W/cm^2),[24] which indicates that in the infrared wavelength range, the absorption is difficult to be bleached, and the perovskites are supposed to have promising application in Q-switching as optical modulators for the generation of pulsed lasers with large pulses based on the theory of passively modulated pulsed lasers.[25] The saturable absorption can also be qualitatively understood based on the electronic band gap structure.[21]

When the samples are irradiated by weak light at 1064 nm, rather than be transferred from valence band to the conduction band, the photoexcited electrons would be trapped by the subgap trap states within the bandgap and will depopulate in the time scale of 100 μs to 1 ms subsequently.[21] However, under high intensity irradiation, the final electronic states will be fully occupied, blocking further absorption and transition from the valence to the subgap trap states, which induces the samples to exhibit saturable absorption in the time shorter than the recombination lifetime especially under the pump lasers with the pulse width of 40 ps.

Unlike the two-photon absorption in the near-infrared wavelength band of a single crystal $CH_3NH_3PbBr_3$ reported recently,[26] the saturable absorption of perovskites in our work

DOI: 10.1021/acsphotonics.5b00563
ACS Photonics 2016, 3, 371−377

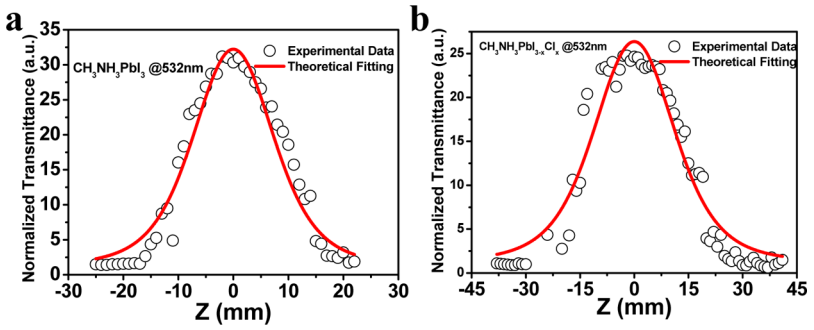

Figure 4. Nonlinear absorption of $CH_3NH_3PbI_3$ and $CH_3NH_3PbI_{3-x}Cl_x$ samples in open aperture condition under irradiation of a 532 nm pulsed laser. (a) Experimental results and theoretical fitting for the nonlinear absorption of $CH_3NH_3PbI_3$. (b) Experimental results and theoretical fitting for the nonlinear absorption of $CH_3NH_3PbI_{3-x}Cl_x$.

should be generated by the distribution of subgap trap states, and has the nonlinear absorption coefficient of 3 orders of magnitude larger than that of two absorption coefficient of $CH_3NH_3PbBr_3$ single crystal (8.2 cm/GW) as shown in Table 1. To rule out the possibility of contributions from PbI_2 from incomplete reaction or degradation of the perovskite film, we have measured the structures of the perovskite samples before and after the Z-scan and laser experiments by X-ray diffraction measurement. The results are shown in the Supporting Information, which shows that there was no PbI_2 from incomplete reaction or degradation of the perovskite film. We show the experimental results of the nonlinear transmission at the irradiation wavelength of 1064 nm in the close aperture condition in Figure 3, panels c and d for $CH_3NH_3PbI_3$ and $CH_3NH_3PbI_{3-x}Cl_x$, respectively. Via the theoretical fitting of the experimental results, the procedure for which we describe in Supporting Information, we obtain a NRI of $\gamma = 3.74 \times 10^{-15}$ m^2/W for $CH_3NH_3PbI_3$, and $\gamma = 8.36 \times 10^{-15}$ m^2/W for $CH_3NH_3PbI_{3-x}Cl_x$. The nonlinear refractive index of the perovskites is therefore, respectively, 10^3 and 10^2 times larger than those of Si ($\gamma = 4.5 \times 10^{-18}$ m^2/W)[13] and GaAs ($\gamma = 3.25 \times 10^{-17}$ m^2/W),[27] both of which have been identified as excellent absorbers in solar cells and exciting materials for nonlinear optoelectronics, and is 10^5 times larger than that of silica ($\gamma = 2 \times 10^{-20}$ m^2/W),[28−30] which has been extensively applied in the nonlinear waveguides in the advantages of sizes and easiness of preparation. On the basis of nonlinear optical theory, it can be derived that the distortion of electron clouds and the rotation of molecular dipoles formed by the CH_3^+ and NH_2^- taking place in few picoseconds[31−33] are responsible for this nonlinear optical response of refractive index on the incident pump power. The difference of NRI indicates that the introduction of Cl^- ions, or the impact this has on the formed perovskite crystals, by some means, results in a slight structural destabilization leading to the redistribution of the delocalized electrons in $CH_3NH_3PbI_{3-x}Cl_x$, just like the difference of NRI between fullerene C_{60} and its derivatives.[34] Compared with $CH_3NH_3PbI_3$, we can get that the contribution of distorted octahedral to the NRI is $\gamma = 4.62 \times 10^{-15}$ m^2/W larger than that of $CH_3NH_3PbI_3$, which confirms that the conduction and valence band are predominately determined by the PbI_4X_2 (with X = Cl or I) octahedral in agreement with the theoretical calculation,[16] and displays that electrons in $CH_3NH_3PbI_{3-x}Cl_x$ films are much more weakly bound than those in $CH_3NH_3PbI_3$. Moreover, the large NRIs of the two perovskites indicate that their refractive indexes are sensitive to the intensity of light and should have promising applications in optoelectronics such as optical modulation, frequency-shifting by four-wave mixing, or Raman effects[13,35,36] as tens of times more sensitive devices.

In the sunlight spectra, the peak intensity is located at about 500 nm, where light absorption promotes band gap transition. The nonlinear absorption at this wavelength band is important for discovering the nature in a solar cell and might be helpful for understanding if there is an influence of the rotation of molecular dipoles forming the CH_3^+ and NH_2^- in possible ferroelectric domains upon the absorption coefficient in the perovskite solar cells. With the frequency doubling of the pump source by employing a potassium titanium oxygenic phosphate (KTP) single crystal, we realized a 532 nm pulsed laser for the investigation of nonlinear absorption. We show the results of nonlinear absorption of $CH_3NH_3PbI_3$ and $CH_3NH_3PbI_{3-x}Cl_x$ in Figure 4a,b. Fitting the experimental results, we determine the nonlinear absorption coefficient with $\beta = -152$ cm/MW and saturable intensity of $I_{sat} = 0.84$ GW/cm^2 for $CH_3NH_3PbI_3$ and $\beta = -203.3$ cm/MW and $I_{sat} = 0.5$ GW/cm^2 for $CH_3NH_3PbI_{3-x}Cl_x$. In the present studied time scales, the laser generates the electrons that transfer from valence band to conduction band and the local field may also induce an orientation of the molecular dipoles. The influence of the two effects above on the absorption of the perovskites is shown as the nonlinear absorption coefficient. Under irradiation by simulated sunlight (AM 1.5), the generated carrier intensity can be calculated with the rate equation:[37]

$$N_{carrier} = \frac{\alpha I \tau}{h\omega} \tag{4}$$

where τ is the carrier recombination time and h is the Planks constant. On the basis of eqs 2 and 4, the carrier densities with and without nonlinear absorption show almost no change with the values of 0.26×10^{15} cm^3 for $CH_3NH_3PbI_3$ and 7.3×10^{15} cm^3 for $CH_3NH_3PbI_{3-x}Cl_x$ which shows that the carrier density of $CH_3NH_3PbI_{3-x}Cl_x$ is about 30 times larger than that of $CH_3NH_3PbI_3$ under same irradiation due to the difference in the carrier recombination lifetime.[4] To obtain a 10% change in absorption, reduction of absorption coefficients, due to the nonlinear effects, we would need to increase the solar intensity to be about 132 and 222 MW/cm^2 for $CH_3NH_3PbI_3$ and $CH_3NH_3PbI_{3-x}Cl_x$, respectively. The results also denote that the orientation of molecular dipoles in the perovskites has almost no influence on the absorption and photon generated carrier concentrations when they are applied as absorbers in solar cells, which are in agreement with the recent reported result in perovskites solar cells.[38] Therefore, the influence of carrier intensity induced by the orientating of the molecular

DOI: 10.1021/acsphotonics.5b00563
ACS Photonics 2016, 3, 371−377

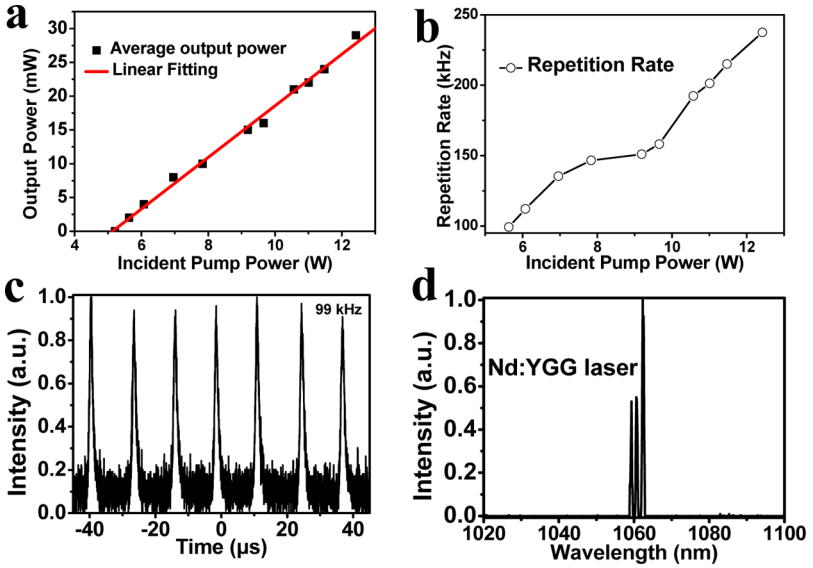

Figure 5. Pulsed laser performance with $CH_3NH_3PbI_3$ as the optical modulator at 1.06 μm. (a) Average output power with the increase of incident pump power with the threshold of 5.2 W. (b) Repetition rate with the increase of incident pump power in the range from 99 to 237 kHz. (c) Pulse train with the repetition rate of 99 kHz and pulse width of 660 ns. (d) Modulated pulsed Nd:YGG laser spectra.

dipoles on the hysteresis effect could be ruled out, consistent with the hysteresis in the solar cells primarily originating from macroscopic polarization due to the presence of mobile ionic species.[34]

Passively Q-Switched Laser. On the basis of the measurement of nonlinear response, here we demonstrate the application as a pulsed modulator in solid-state lasers at 1.06 μm. We show the output power and repetition rate with the incident pump power in Figure 5a,b. We observe that the output power and repetition rate increase with the pump power giving the maximum output power of 29 mW in the range of 99−237 kHz and the temporal pulse width decreases from 660 to 305 ns. These results are typical for passive Q-switching. We show the typical pulse train with a repetition rate of 99 kHz under the pump power of 5.6 W in Figure 5c. On the basis of the average output power repetition rate, we calculate the pulse energy with a maximum value of about 131 nJ with the laser wavelength located at 1.06 μm as shown in Figure 5d. These results have been obtained in a simple spin-coated thin film on a glass substrate. It is likely that the result can be substantially improved by further optimization in the modulation depth of the perovskites, the doping concentration or tuning of the composition of the crystal and designing of a laser cavity.

CONCLUSIONS

We have investigated the nonlinear optical response of the organic−inorganic perovskites absorbers $CH_3NH_3PbI_3$ and $CH_3NH_3PbI_{3-x}Cl_x$ including the NRI and nonlinear optical absorption coefficient induced by the real and imaginary parts of third-order nonlinear dielectric permittivity, respectively. Our detailed comparisons among organic−inorganic perovskites with Si, silica, and GaAs, which are presented in Table 1, show that the perovskites have large NRI and saturable absorption properties, suggesting it has promising applications in the generation of pulsed lasers. The breaking of PbI_4X_2 (with X = Cl or I) octahedral symmetry with introduction of Cl anions could be responsible for the larger NRI of $CH_3NH_3PbI_{3-x}Cl_x$ compared with that of $CH_3NH_3PbI_3$ and indicates the strong tenability of perovskite semiconductors by subtle variations in composition. On the basis of the nonlinear optical response, we demonstrated a pulsed IR laser with the perovskites as an optical modulator. All of these results identify the perovskites as also having promising applications in other optoelectronics in addition to the extensively studied solar cells and the presented optical modulator.

EXPERIMENTAL METHODS

Material Preparation. In the present study, a set of commercial far-ultraviolet quartz glass wafers ($\Phi 25 \times 1$ mm^3) were employed as the substrates, which were polished and uncoated. Both the $CH_3NH_3PbI_3$ and $CH_3NH_3PbI_{3-x}Cl_x$ thin films were deposited on the substrates by a solution-processed method in Supporting Information. In particular, the $CH_3NH_3PbI_3$ thin film was obtained by a sequential deposition method, and the $CH_3NH_3PbI_{3-x}Cl_x$ thin film was prepared by simply mixing the $PbCl_2$ and CH_3NH_3I precursor solution with a ratio of 1:3. The thickness of perovskite thin films was controlled to be around 400 nm. Top-down scanning electron microscope (SEM) images of as-prepared perovskite thin films were characterized by a field emission scanning electron microscopy (JEOL JSM-7500F) (Figure S1).

Laser Design. A fiber-coupled diode laser was employed as the pump source with the emission of 808 nm. A neodymium doped yttrium gallium garnet Nd:$Y_3Ga_5O_{12}$ (Nd:YGG) single crystal was used as the gain material cut along the <111> direction with the dimensions of 3 mm × 3 mm × 6 mm. The neodymium doping concentration was 1 at%. The detailed description for the laser configuration is shown in the Supporting Information. The $CH_3NH_3PbI_3$ was inserted into the two-mirror resonator near the concave output coupler in case the pump light influenced the optical switching performance.

ASSOCIATED CONTENT

Supporting Information

The Supporting Information is available free of charge on the ACS Publications website at DOI: 10.1021/acsphotonics.5b00563.

DOI: 10.1021/acsphotonics.5b00563
ACS Photonics 2016, 3, 371−377

The detailed preparation processes of perovskites absorbers $CH_3NH_3PbI_3$ and $CH_3NH_3PbI_{3-x}Cl_x$ thin film, the experimental setup for Z-scan technique, and the detailed description for the laser configuration with perovskite as optical modulator; structures of the perovskite thin films before and after the Z-scan and laser experiments. (PDF)

AUTHOR INFORMATION

Corresponding Authors

*E-mail: haohaiyu@sdu.edu.cn.
*E-mail: huaijinzhang@sdu.edu.cn.
*E-mail: h.snaith1@physics.ox.ac.uk.

Author Contributions

#R.Z. and J.F. contributed equally to this work.

Notes

The authors declare no competing financial interest.

ACKNOWLEDGMENTS

The research was supported by the National Natural Science Foundation of China (Nos. 51422205 and 51272131), "973 program" early projects (No. 2014CB260405), "Advanced Talents Program of Hebei Province (No. GCC2014013) and Natural Science Foundation for Distinguished Young Scholars of Shandong Province (JQ201415). Top Young Outstanding Innovative Talents Program of Hebei Province (No. BJ2014009), Natural Science Foundation of Hebei Province (No. F2015201189), "100 Talents Program of Hebei Province" (E2014100008). J. Fan also thanks the support of the Secretary for Universities and Research of the Ministry of Economy and Knowledge of the Government of Catalonia. This work was part funded by the Engineering and Physical Sciences Research Council (EPSRC), U.K.

REFERENCES

(1) Heo, J. H.; Im, S. H.; Noh, J. H.; Mandal, T. N.; Lim, C.-S.; Chang, J. A.; Lee, Y. H.; Kim, H.-J.; Sarkar, A.; Nazeeruddin, M. K. Efficient Inorganic-Organic Hybrid Heterojunction Solar Cells Containing Perovskite Compound and Polymeric Hole Conductors. *Nat. Photonics* **2013**, *7*, 486−491.

(2) Green, M. A.; Emery, K.; Hishikawa, Y.; Warta, W.; Dunlop, E. D. Solar Cell Efficiency Tables (version 39). *Prog. Photovoltaics* **2012**, *20*, 12−20.

(3) Kojima, A.; Teshima, K.; Shirai, Y.; Miyasaka, T. Organometal Halide Perovskites as Visible-Light Sensitizers for Photovoltaic Cells. *J. Am. Chem. Soc.* **2009**, *131*, 6050−6051.

(4) Stranks, S. D.; Eperon, G. E.; Grancini, G.; Menelaou, C.; Alcocer, M. J.; Leijtens, T.; Herz, L. M.; Petrozza, A.; Snaith, H. J. Electron-Hole Diffusion Lengths Exceeding 1 Micrometer in an Organometal Trihalide Perovskite Absorber. *Science* **2013**, *342*, 341−344.

(5) Lee, M. M.; Teuscher, J.; Miyasaka, T.; Murakami, T. N.; Snaith, H. J. Efficient Hybrid Solar Cells Based on Meso-Superstructured Organometal Halide Perovskites. *Science* **2012**, *338*, 643−647.

(6) Burschka, J.; Pellet, N.; Moon, S.-J.; Humphry-Baker, R.; Gao, P.; Nazeeruddin, M. K.; Grätzel, M. Sequential Deposition as a Route to High-Performance Perovskite-Sensitized Solar Cells. *Nature* **2013**, *499*, 316−319.

(7) Liu, M.; Johnston, M. B.; Snaith, H. J. Efficient Planar Heterojunction Perovskite Solar Cells by Vapour Deposition. *Nature* **2013**, *501*, 395−398.

(8) Mei, A.; Li, X.; Liu, L.; Ku, Z.; Liu, T.; Rong, Y.; Xu, M.; Hu, M.; Chen, J.; Yang, Y. A Hole-Conductor-Free, Fully Printable Mesoscopic Perovskite Solar Cell with High Stability. *Science* **2014**, *345*, 295−298.

(9) Zhou, H.; Chen, Q.; Li, G.; Luo, S.; Song, T.-B.; Duan, H.-S.; Hong, Z.; You, J.; Liu, Y.; Yang, Y. Photovoltaics Interface Engineering of Highly Efficient Perovskite Solar Cells. *Science* **2014**, *345*, 542−546.

(10) Jeon, N. J.; Noh, J. H.; Yang, W. S.; Kim, Y. C.; Ryu, S.; Seo, J.; Seok, S. I. Compositional Engineering of Perovskite Materials for High-Performance Solar Cells. *Nature* **2015**, *517*, 476−480.

(11) Green, M. A.; Ho-Baillie, A.; Snaith, H. J. The Emergence of Perovskite Solar Cells. *Nat. Photonics* **2014**, *8*, 506−514.

(12) van Reenen, S.; Reenen, S.; Kemerink, M.; Snaith, H. J. Modeling Anomalous Hysteresis in Perovskite Solar Cells. *J. Phys. Chem. Lett.* **2015**, *6*, 3808−3814.

(13) Leuthold, J.; Koos, C.; Freude, W. Nonlinear Silicon Photonics. *Nat. Photonics* **2010**, *4*, 535−544.

(14) Tan, Z.-K.; Moghaddam, R. S.; Lai, M. L.; Docampo, P.; Higler, R.; Deschler, F.; Price, M.; Sadhanala, A.; Pazos, L. M.; Credgington, D. Bright Light-Emitting Diodes Based on Organometal Halide Perovskite. *Nat. Nanotechnol.* **2014**, *9*, 687−692.

(15) Hu, X.; Zhang, X.; Liang, L.; Bao, J.; Li, S.; Yang, W.; Xie, Y. High-Performance Flexible Broadband Photodetector Based on Organolead Halide Perovskite. *Adv. Funct. Mater.* **2014**, *24*, 7373−7380.

(16) Dhanker, R.; Brigeman, A.; Larsen, A.; Stewart, R.; Asbury, J.; Giebink, N. Random Lasing in Organo-Lead Halide Perovskite Microcrystal Networks. *Appl. Phys. Lett.* **2014**, *105*, 151112.

(17) Mosconi, E.; Amat, A.; Nazeeruddin, Md. K.; Grätzel, M.; De Angelis, F. First-Principles Modeling of Mixed Halide Organometal Perovskites for Photovoltaic Applications. *J. Phys. Chem. C* **2013**, *117*, 13902−13913.

(18) Baikie, T.; Fang, Y.; Kadro, J. M.; Schreyer, M.; Wei, F.; Mhaisalkar, S. G.; Graetzel, M.; White, T. J. Synthesis and Crystal Chemistry of the Hybrid Perovskite $(CH_3NH_3)PbI_3$ for Solid-State Sensitised Solar Cell Applications. *J. Mater. Chem. A* **2013**, *1*, 5628−5641.

(19) Fang, Y.; Dong, Q.; Shao, Y.; Yuan, Y.; Huang, J. Highly Narrowband Perovskite Single-Crystal Photodetectors Enabled by Surface-Charge Recombination. *Nat. Photonics* **2015**, *9*, 679−686.

(20) Wang, X.; Wang, P.; Wang, J.; Hu, W.; Zhou, X.; Guo, N.; Huang, H.; Sun, S.; Shen, H.; Lin, T.; Tang, M.; Liao, L.; Jiang, A.; Sun, J.; Meng, X.; Chen, X.; Lu, W.; Chu, J. (2015). Ultrasensitive and Broadband MoS_2 Photodetector Driven by Ferroelectrics. *Adv. Mater.* **2015**, *27*, 6575−6581.

(21) Stranks, S. D.; Burlakov, V. M.; Leijtens, T.; Ball, J. M.; Goriely, A.; Snaith, H. J. Recombination Kinetics in Organic-Inorganic Perovskites: Excitons, Free Charge, and Subgap States. *Phys. Rev. Appl.* **2014**, *2*, 034007.

(22) Sheik-Bahae, M.; Said, A. A.; Wei, T. H.; Hagen, D. J.; Van Stryland, E. W. Sensitive Measurement of Optical Nonlinearities Using a Single Beam. *IEEE J. Quantum Electron.* **1990**, *26*, 760−769.

(23) Petit, Y.; Joly, S.; Segonds, P.; Boulanger, B. Recent Advances in Monoclinic Crystal Optics. *Laser Photon. Rev.* **2013**, *7*, 920−937.

(24) Bao, Q. L.; Zhang, H.; Wang, Y.; Ni, Z.; Yan, Y.; Shen, Z. X.; Loh, K. P.; Tang, D. Y. Atomic-Layer Graphene as a Saturable Absorber for Ultrafast Pulsed Lasers. *Adv. Funct. Mater.* **2009**, *19*, 3077−3083.

(25) Keller, U. Recent Developments in Compact Ultrafast Lasers. *Nature* **2003**, *424*, 831−838.

(26) Walters, G.; Sutherland, B. R.; Hoogland, S.; Shi, D.; Comin, R.; Sellan, D. P.; Bakr, O. M.; Sargent, E. H. Two-Photon Absorption in Organometallic Bromide Perovskites. *ACS Nano* **2015**, *9*, 9340−9346.

(27) Xie, G.; Tang, D.; Kong, J.; Qian, L. Passive Mode-Locking of a Nd:YAG Ceramic Laser by Optical Interference Modulation in a GaAs Wafer. *Opt. Express* **2007**, *15*, 5360−5365.

(28) Ferrera, M.; Razzari, L.; Duchesne, D.; Morandotti, R.; Yang, Z.; Liscidini, M.; Sipe, J. E.; Chu, S.; Little, B. E.; Moss, D. J. Low-Power Continuous-Wave Nonlinear Optics in Doped Silica Glass Integrated Waveguide Structures. *Nat. Photonics* **2008**, *2*, 737−740.

(29) Liu, A. C.; Digonnet, M. J. F.; Kino, G. S. Measurement of the dc Kerr and Electrostrictive Phase Modulation in Silica. *J. Opt. Soc. Am. B* **2001**, *18*, 187−194.

DOI: 10.1021/acsphotonics.5b00563
ACS Photonics 2016, 3, 371−377

(30) Szameit, A.; Burghoff, J.; Pertsch, T.; Nolte, S.; Tünnermann, A.; Lederer, F. Two-Dimensional Soliton in Cubic fs Laser Written Waveguide Arrays in Fused Silica. *Opt. Express* **2006**, *14*, 6055−6062.
(31) Quarti, C.; Mosconi, E.; De Angelis, F. Interplay of Orientational Order and Electronic Structure in Methylammonium Lead Iodide: Implications for Solar Cell Operation. *Chem. Mater.* **2014**, *26*, 6557−6569.
(32) Wasylishen, R. E.; Knop, O.; MacDonald, J. B. Cation Rotation in Methylammonium Lead Halides. *Solid State Commun.* **1985**, *56*, 581−582.
(33) Poglitsch, A.; Weber, D. Dynamic Disorder in Methylammoniumtrihalogenoplumbates (II) Observed by Millimeterwave Spectroscopy. *J. Chem. Phys.* **1987**, *87*, 6373−6378.
(34) Wang, P.; Ming, H.; Xie, J.; Zhang, W.; Gao, X.; Xu, Z.; Wei, X. Substituents Effect on the Nonlinear Optical Properties of C_{60} Derivatives. *Opt. Commun.* **2001**, *192*, 387−391.
(35) Frost, J. M.; Butler, K. T.; Brivio, F.; Hendon, C. H.; Van Schilfgaarde, M.; Walsh, A. Atomistic Origins of High-Performance in Hybrid Halide Perovskite Solar Cells. *Nano Lett.* **2014**, *14*, 2584−2590.
(36) Rong, H.; Jones, R.; Liu, A.; Cohen, O.; Hak, D.; Fang, A.; Paniccia, M. A Continuous-Wave Raman Silicon Laser. *Nature* **2005**, *433*, 725−728.
(37) Garmire, E. Resonant Optical Nonlinearities in Semiconductors. *IEEE J. Sel. Top. Quantum Electron.* **2000**, *6*, 1094−1110.
(38) Xiao, Z.; Yuan, Y.; Shao, Y.; Wang, Q.; Dong, Q.; Bi, C.; Sharma, P.; Gruverman, A.; Huang, J. Giant Switchable Photovoltaic Effect in Organometal Trihalide Perovskite Devices. *Nat. Mater.* **2015**, *14*, 193−198.

DOI: 10.1021/acsphotonics.5b00563
ACS Photonics 2016, 3, 371−377